Farhana *et al. Sustainable Energy Research* (2024) 11:1
https://doi.org/10.1186/s40807-023-00090-z

Sustainable Energy Research

ORIGINAL RESEARCH ARTICLE **Open Access**

Noble MXene nanofluids' impact on solar collector effectiveness enhancement: a CFD numerical evaluation

Kaniz Farhana[1,2*], Abu Shadate Faisal Mahamude[3], Kumaran Kadirgama[3,4] and Rajan Jose[5,6]

Abstract

The thermal flat plate solar collector (FPSC) is a versatile solar harvesting system that may be integrated into various designs and base fluids. This study presents a novel investigation of using nanofluids to transfer thermal energy in an FPSC system. Using the governing equations in CFD simulations, the performance of an FPSC is studied numerically. The base fluid has been defined as a 60:40 blend of ethylene glycol and water. The effects of three distinct volume fractions of MXene nanofluids in the 0.01–0.1% range on the efficiency are investigated. The numerical findings revealed that employing MXene nanofluid increases outlet temperature efficiency by about 5.83%, 6.06%, and 6.31% when 0.01%, 0.05%, and 0.1% volume fractions of nanofluids are used, respectively. The research aims to create a validated numerical model that can be used to assess the effectiveness of FPSC utilizing ethylene glycol and water or other nanofluids of any mass fraction as a working fluid. To examine the overall effectiveness of the FPSC, a numerical model was created using Solidworks software and ANSYS ICEM CFD. The numerical findings revealed that (i) increasing the proportion of MXene nanofluid in the FPCS enhances efficiency to 0.1% volume fraction, and (ii) MXene nanoparticles may be used in the solar collector to improve efficiency.

Keywords MXene, Nanofluids, ANSYS, Solar Collector, Efficiency

Introduction

The massive need for efficient energy use contributes to a global energy crisis and the depletion of fossil fuel reserves. To identify enough renewable energy sources to address the world's energy needs, a terrible study is currently being done (Chu et al., 2017). The scientific community is paying more attention to renewable energy supplies because of their environmentally beneficial practices rather than natural fossil fuels (Zaman & Abd-el Moemen, 2017). Solar energy is the oldest, most plentiful, transparent, practical, and ecologically friendly renewable natural resource. It is also the most commonly used source for generating heat for home and industrial uses (Bagherian & Mehranzamir, 2020; Fernández-García et al., 2010). A flat plate solar collector (FPSC) is one of the most common solar energy harvesting devices to convert solar irradiation into heat for solar energy systems. Solar harvesting devices are primarily used to change high-energy solar radiation into thermal energy (Farhana, Mahamude, et al., 2019c; Rehan et al., 2018; Sahin et al., 2020). In general, header and riser tubes are the essential parts of FPSC to

*Correspondence:
Kaniz Farhana
kanizfar7@gmail.com; kaniz.farhana@butex.edu.bd
[1] Department of Apparel Engineering, Bangladesh University of Textiles, Dhaka 1208, Bangladesh
[2] Department of Mechanical & Aerospace Engineering, George Washington University, Washington, DC, USA
[3] Faculty of Mechanical and Automotive Engineering Technology, Universiti Malaysia Pahang Al-Sultan Abdullah, 26600 Pekan, Pahang, Malaysia
[4] College of Engineering, Almaaqal University, Basra 61003, Iraq
[5] Faculty of Industrial Science & Technology, Universiti Malaysia Pahang Al-Sultan Abdullah, 26100 Gambang, Malaysia
[6] Center of Intelligent Materials, University Malaysia Pahang, 26300 Kuantan, Malaysia

absorb solar radiation and enhance the heat-generating rate. Working fluids inside flow through the tube aid in absorbing more solar irradiation to increase the thermal energy-producing rate of FPSC (Ahmadlouydarab et al., 2020; Farhana, Kadirgama, & Noor, 2021b). However, this technology is not sufficient to escalate the efficiency of FPSC. Many empirical and experimental investigations have been conducted to improve the thermal efficiency of FPSC in various aspects (Abu-Hamdeh et al., 2021; Farhana et al., 2021a, 2021b; Farhana, Kadirgama, & Noor, 2021b). Transforming the newly outstanding nanofluid in replacement of the conventional working fluid is one of the most contemporary research activities to raise the thermal efficiency of FPSC (Farhana, Kadirgama, Rahman, et al., 2019a, 2019b, 2019c). Nanofluids are the new generation fluids that have superb capabilities to impact any heat-developing device effectively. Minuscule elements in nano-sized shapes (Metallic: Ag, Al, Cu, Au; non-metallic: Al_2O_3, CuO, TiO_2, ZnO; carbon nanotubes: SWCNT, MWCNT, etc.) dispersed into the working fluids (Water, ethylene glycol, thermal oil, etc.) prepared the expected fluids coined as nanofluids. The aforementioned nanoparticles and/or nanofluids have already been utilized in FPSC to increase their effectiveness, according to various types of literature. To perform theoretical and experimental investigations, a variety of mono and hybrid nanofluids have been chosen at varied mass fractions (Borode et al., 2019; Verma et al., 2020; Yusaf et al., 2022). In one of our previous theoretical studies, Farhana, Kadirgama, Noor, et al. (2019a) found the significance of mono (Al_2O_3, TiO_2, ZnO) and hybrid (ZnO + Al_2O_3, Al_2O_3 + TiO_2, TiO_2 + ZnO,) nanofluids in FPSC concerning with various aspects, such as velocity magnitude, turbulence kinetic energy, and dynamic pressure. Header (Fixed in number with two) and a various number of riser tubes had been used to prepare a complete FPSC to investigate the behavior and the implications of mono and hybrid nanofluids as well. Empirical examination stated that mono and hybrid nanofluids had a maximum dynamic pressure of 48% and 16%, respectively; velocity magnitude was about 1.2% and 5.8% for mono and hybrid nanofluids, respectively; and finally, mono and hybrid nanofluids had a top position of 5.5% and 18%, respectively. In a recent study, Ahmadlouydarab et al. (2022) examined the thermal efficiency of FPSC using TiO_2 nanofluids at two kinds of mass fractions such as 0.25% and 1% experimentally. The authors employed two FPSCs and one of them had a larger plate area, the cylindrical solar collector (CSC) was also used in this study. Thermal efficacy tests were performed in 120 and 240 min heat absorption and 180 and 240 min heat retention durations. The authors found the thermal efficiency of 49.61%, 58.00%, and 34.23% using nanofluids with a mass concentration of 0.25% and finally, the thermal efficiencies of 54.86%, 63.67%, and 39.89% were revealed using with a mass concentration of 1% for CSC, small FPSC, and substantial FPSC, respectively, to demonstrate an upsurge in the thermal efficiency of FPSC. In another study, Mahamude et al. (2022) examined the efficacy of FPSC by employing 0.1%, 0.3%, and 0.5% vol. fraction of mono CNC (Produced from waste cotton), reduced graphene and hybrid (CNC+ graphene) nanofluids under direct solar irradiation at fixed mass flow rate. The thermal efficacy of the FPSC is remarkably increased with 0.5% vol. concentration of hybrid (CNC+ graphene) nanofluids.

Recently invented novel 2D transition metal carbides and nitrides drew tremendous attention of the researcher to explore it fully after the first devised by Naguib et al. (2011) and coined as MXene. The fundamental chemical formula of MXene is $M_{n+1}AX_n$; where M stands as an early transition metal, such as Ta, Sc, V, Mo, W, Hf, Ti, Nb, Cr, Zr, etc.; X defines nitrogen and/or carbide and A is the interleaved layer between M and X; n denotes a range of 1 to 3 (Shekhirev et al., 2021). Many studies reported that MXenes have excellent properties such as tunable terminators, metallic conductivity, higher chemical surface area, and superb processability which attained the attraction of researchers to explore them as versatile nanomaterials to fix enormous applications fields, such as energy, wastewater treatment, intelligent textiles, biomedical, and so on (Sajid, 2020; Sreedhar & Noh, 2021). Moreover, due to the inherent structure of MXene nanomaterials exhibit excellent thermal conductivity. The MXene structure offers them a special selection of property tailoring through compositional change due to the diverse choices of M and X ions. As it is formed, MXene has an electrical conductivity of ~ 9.1 S cm^{-1}, making it a highly electrically conductive substance (Farhana et al., 2023; Yin et al., 2022). The thermal conductivity of MXene film had been investigated by Chen et al. (2018) and it had been revealed the magnificent improvement of thermal conductivity from 1.26 W/m. K at 80 K to 2.84 W/m. K at 290 K in the film of MXene. On the other hand, thermal conductivity is one of the most imperative properties to enhance the efficacy of any energy device, such as PV/T (Rubbi et al., 2020), solar dish collector (Aslfattahi et al., 2021), direct absorption solar collector Li et al. (2020), etc. In one study, Samylingam et al. (2020), revealed the thermal efficacy enhancement of PV/T of about 16% at a 0.07 kg/s mass flow rate compared with Al_2O_3–water nanofluids by applying MXene nanofluid. Besides, the heat transfer coefficient raised to 9% for MXene nanofluid. There is, nevertheless, a need to investigate the effectiveness of

FPSC employing MXene nanofluids. As a result, there is a huge opportunity to investigate how MXene-based nanofluids can improve FPSC efficiency both theoretically and experimentally. Therefore, this article shows the thermal efficacy of FPSC has been performed theoretically using ethylene glycol–water (60:40) MXene-based nanofluids. ANSYS ICEM CFD was used to simulate the PFSC performance with MXene nanofluids. Before commencement of experimental works, theoretical experience of a research study is more reliable and appropriate to deduct the cost of the experimental works (Koziel & Yang, 2011).

Physical features of MXene nanofluids and relevant mathematical models

MXene

The newly invented MXene is the most impressive 2D material and attracting more attention from scientists and researchers owing to its outstanding chemical, mechanical, and electrical characteristics. Besides, MXene shows good performance as a semiconductor. Due to the existence of ample functional groups (-O, -F, or -OH) and wider surface area that makes it is the most demandable and dynamic material in nanofluid technology. Most importantly, MXene also exhibits notable thermal stability performance, even though a few studies have been conducted on it. Liu and Li (2018) conducted the thermal conductivity measurement of MXene-based nanocomposite and reported excellent output for the efficacy enhancement of energy storage. Several computational equations are employed to compute the fundamental thermophysical features before performing the numerical calculations on the ANSYS workbench. Herein, to fulfill the objectives of this study, a mixture of ethylene glycol and water (60:40) (Farhana et al., 2020) has been considered as the working fluid to prepare the required volumetric concentration of MXene nanofluids, such as 0.01%, 0.05%, and 0.1%. Thermal conductivity, density, and viscosity have been calculated using Eq. (1), (2), and (3) respectively, and these empirical values are tabulated in Table 1:

$$\frac{k_{nf}}{k_{bf}} = \frac{k_{np} + 2k_{bf} + 2\phi\left(k_{np} - k_{bf}\right)}{k_{np} + 2k_{fbf} - \phi\left(k_{np} - k_{bf}\right)} \tag{1}$$

$$\rho_{nf} = \varphi\rho_{np} + (1-\varphi)\rho_{bf} \tag{2}$$

$$\mu_{nf} = \mu(1 + 2.5\phi) \tag{3}$$

Where as k, ρ, and μ stand for thermal conductivity, density, and viscosity, respectively; subscript *np*, *bf*, and *nf* determine nanoparticle, base fluid, and nanofluid, respectively, as well. Besides, one most important mathematical equations has been solved for the specific heat of nanofluids by

Table 1 Properties of MXene nanofluids at various volume concentrations

Properties	0.01% MXene	0.05% MXene	0.1% MXene
Density (kg/m^3)	1046	1048	1050
Specific heat (j/kg. k)	2200	2250	2300
Thermal conductivity (W/m. k)	0.34	0.37	0.45
Viscosity (kg/m. s)	0.0047	0.0053	0.0052

$$C_{p,nf} = \frac{\phi\left(\rho C_p\right)_{np} + (1-\phi)\left(\rho C_p\right)_{bf}}{\rho_{nf}} \tag{4}$$

CFD governing equations

In this study, MXene nanofluids have been preferred as incompressible and the calculated fluid flow was Laminar. The flow rate was 0.0083 kg/s as our investigation was only confined to the efficacy enhancement of solar devices by employing a new MXene nanofluid. Although a lot of studies have been conducted by applying varied types of flow rates and reported superb findings (Farhana, Mahamude, et al., 2019; Yadav & Singh, 2011). The following governing equations are used in CFD simulations (Davarnejad & Jamshidzadeh, 2015; Goodarzi et al., 2014):

Continuity equation

$$\frac{\delta}{\delta_t} = (\rho_m) + \nabla.\left(\rho_m \underset{V_m}{\rightarrow}\right) = 0 \tag{5}$$

Momentum equation

$$\begin{aligned}&\frac{\delta}{\delta_t}\left(\rho_{m\overrightarrow{V_m}}\right) + \nabla.\left(\rho_m \underset{V_m}{\rightarrow}\underset{V_m}{\rightarrow}\right)\\&= -\nabla\rho_m + \nabla.\left[\mu_m\left(\nabla \underset{V_m}{\rightarrow} + \underset{V}{\rightarrow}{}^{T}_{m}\right)\right]\\&+ \rho_m\beta_m(T - T_o)g\end{aligned} \tag{6}$$

Energy equation

$$\frac{\delta}{\delta_t}\rho_m h_m + \nabla.\left(\rho_m h_m \underset{V_m}{\rightarrow}\right) + \nabla.\left(P \underset{V_m}{\rightarrow}\right) = \nabla.\left(K_{eff}\nabla T\right) \tag{7}$$

The efficacy of the solar thermal device has been calculated by the following Eqs. (8) and (9);

$$Q_u = \dot{m}C_p(T_{out} - T_{in}) \tag{8}$$

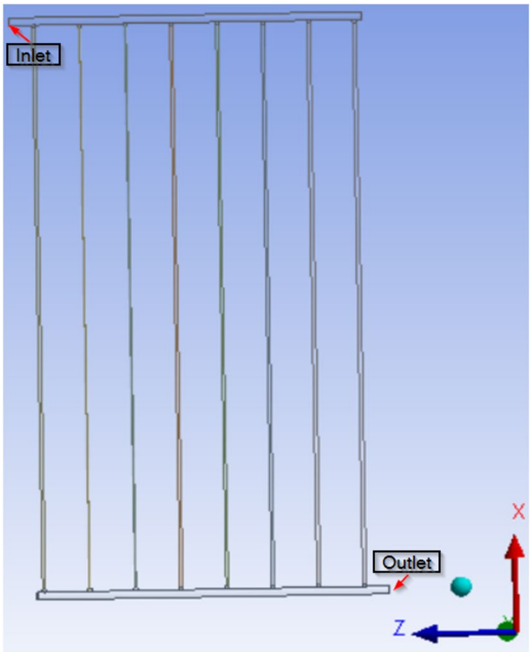

Fig. 1 Schematic geometry of basic design model of header and riser tubes

Table 2 Boundary condition of modelling

Boundary condition	Inlet	Nano	307 K
		Working fluid	0.0083 kg/s (Mass flow rate)
			300 K (Temperature)
	Outlet	Gauge pressure	0 Pa (Pressure)

$$\eta = \frac{Q_u}{I_t A_c} \tag{9}$$

where η is the efficacy; Q_u is the energy gain; T_{out} and T_{in} are the outlet and inlet temperatures, respectively.

Methods

Depiction of project

As shown in Fig. 1, the header and riser pipes of the solar collector were sketched using the SolidWorks software kit using the dimensions from Table 3. Table 3 portrays a complete view of the geometry of FPSC that has been used to simulate the fluid flow through it. EGW as base fluid and MXene/EGW nanofluids were employed at the inlet of the solar collector and the entire description of the boundary conditions of the inlet and outlet of the collector for analysis is listed in Table 2. The most important prerequisites for executing numerical simulations are boundary conditions. The outlet stands after the simulation of fluid flow by moving outside of fluid with zero pressure, while the inlet symbolizes the beginning point of fluid flow that has started at a set mass flow rate and temperature. According to the principle, solar energy absorbed by the header and riser tubes, their conduction of energy occurred from the upper side to the inner side of the tubes; afterward, convection happened with the inside fluids (base and nanofluids) of the tubes. In addition, finally, the fluids transfer the energy to the outlet to increase the efficacy of the solar collector. Herein, the thermal behavior and efficiency of solar collector were studied with the loading of 0.01, 0.05, and 0.1% vol. the concentration of MXene/EGW along with EGW base fluid.

Table 3 Dimension of tubes of solar collector

Parameter	Measurements (mm)
Header tube	Outer diameter 24
	Inner diameter 23.4
	Thickness 0.6
Riser tubes	Outer diameter 11
	Inner diameter 10.55
	Thickness 0.45
Total header length	2000
Total riser length	13,552
No. of header tube	2
No. of riser tubes	8
Materials of the tubes	Copper

Modelling

Only the header and riser tubes of flat plate solar devices were considered in this research. According to the mentioned selected parameters, as illustrated in Table 3; geometry for modelling has been prepared using the SolidWorks software package. Sketching and assembling of geometry preparation are portrayed in Fig. 2 one by one. Besides, the top and front views of the geometry are also presented in Fig. 2. for better visualization of the modelling geometry.

Meshing

Meshing has been done in the ANSYS ICEM CFD module which is suitable for systematic meshing. The refined cutcell mesh has been formed at the boundary in the riser tubes and tetrahedron mesh has been performed in the header tubes. Figure 3b portrays the complete meshed model and Fig. 3a, c shows the enlarged view of the meshed model with refinement. During meshing, the growth rate was 1.2 which was quite good to decline the simulation cost utmost. Afterward, the calculation

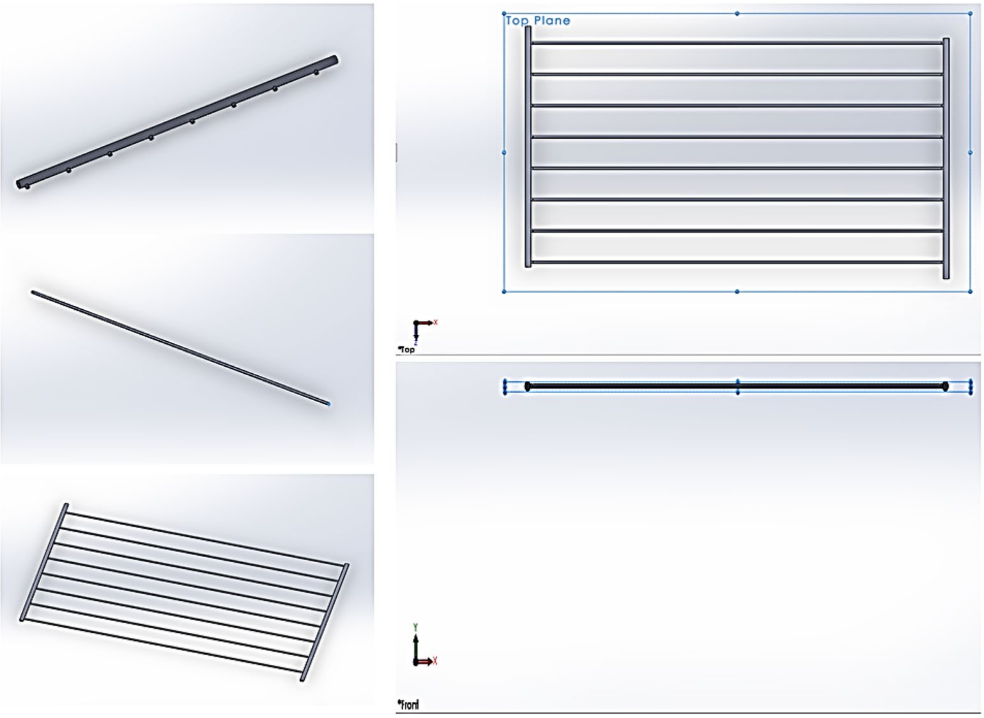

Fig. 2 Stages of geometry preparation with top and front view

solution of the numerical study was performed with 100 iterations, and within this benchmark of iterations, the solutions of all nanofluids have converged, as shown in Fig. 4. Iterations can be varied based on the numerical conditions, but here 100 iterations have been selected as developed solutions obtained within this range.

Study on grid independence

The grid independence study was followed with three different sizes of the mesh, such as coarse, medium, and fine, as tabulated in Table 4. The statistics of the sizes reported similar values between coarse and medium mesh sizes but fine presented higher than the other two. Primarily, the computation performed for a particular fluid using these three mesh sizes individually and the computed data have been studied, as in Table 3. There was not any change in computed date data of the outlet temperature for all sizes of meshes. Therefore, for computation costs and time, coarse-sized meshes were selected for further studies.

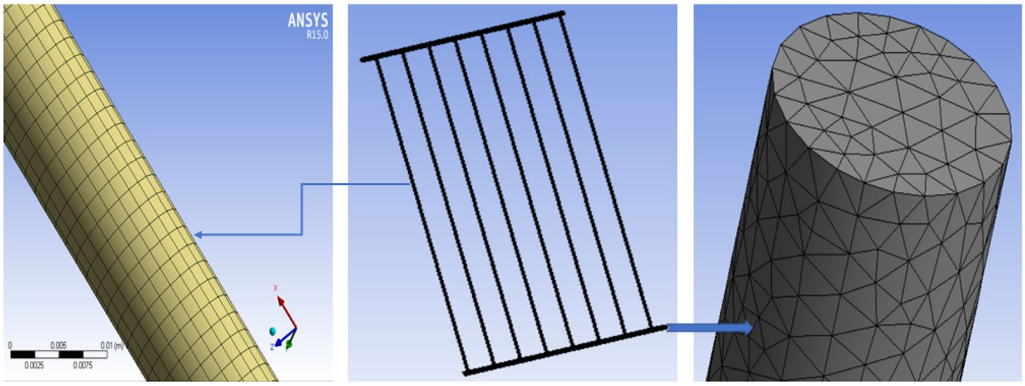

Fig. 3 Meshed model with an enlarged view

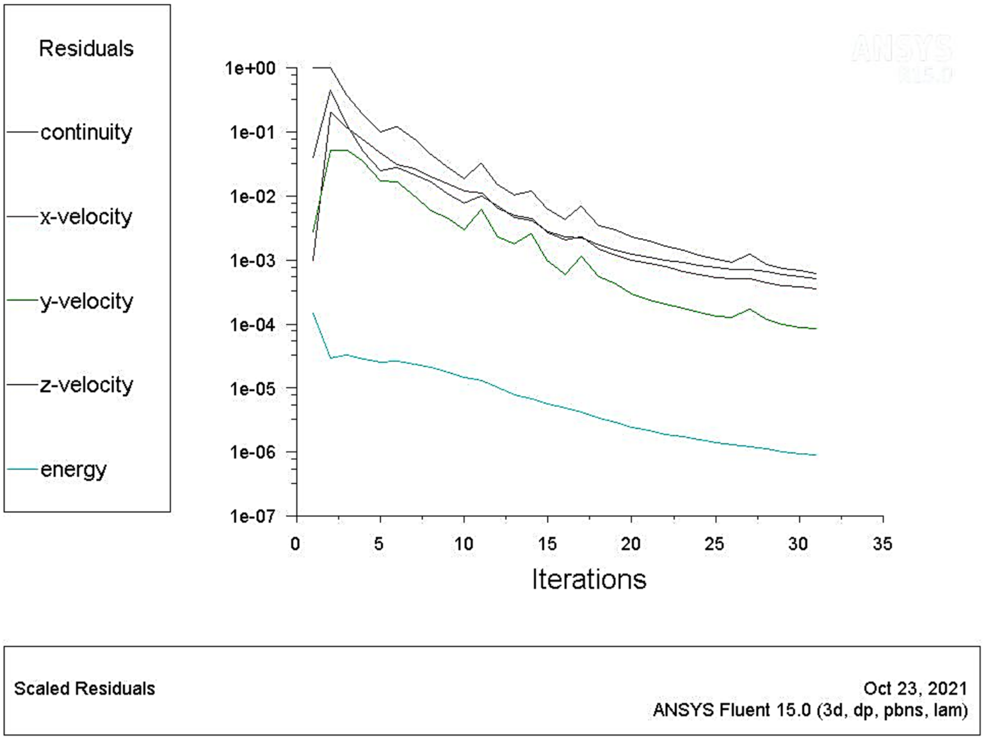

Fig. 4 Scheme of the converged solution

Table 4 Grid independent study

Mesh size	Mesh statistics	Temperature (K)
Coarse	Nodes–626,092 Elements–678,046	305.7
Medium	Nodes–626,092 Elements–678,046	305.7
Fine	Nodes–633,133 Elements–686,547	305.7

Results and discussion

According to the study, Fig. 5 displays the simulation contour of the total temperature for the unique MXene mono nanofluid at a concentration of 0.01% vol. (only 0.01% has been displayed, because all vol. concentrations showed nearly comparable contours). Blue denotes the minimal value in the CFD post-processing phase, while red denotes the highest value and completely completed solution (Sorokes et al., 2016). Furthermore, Mazumder (2012) demonstrated in a study that the solutions evolve gradually from blue to red in the geometric contour, as shown in Fig. 5a. Besides, Fig. 5c shows a fully developed solution at the outlet but merely a solution developed at the inlet of the tubes, as presented in Fig. 5b. As a consequence, the application of novel MXene nanofluids increases the temperature at the outlet in the solar harvesting device, as shown in Fig. 6. Figure 6 depicts the improvement in temperature due to adding MXene nanoparticles into the base fluid. In addition, 0.01%, 0.05%, and 0.1% MXene/EGW nanofluids exhibited the progressive increment of temperature with increasing volume concentrations of nanofluids. This phenomenon is similar to the study of Genc et al., (2018). Herein, the authors revealed numerically that nanofluids as well as increasing volume concentration of nanofluids raise the outlet temperature of flat plate solar collector. To correlate this performance of MXene nanofluids, the temperature behaviour of graphene nanofluids has been studied apparently at similar vol. con., such as 0.01%, 0.05%, and 0.1% which is demonstrated in Fig. 7. In this comparison, study graphene exhibited higher temperature improvement than MXene nanofluids in all volume concentrations. In the case of heat transfer rate, 0.01% and 0.05% vol. the concentration of MXene nanofluids performed the analogous performance of heat transfer rate as portrayed in Fig. 8 excepting 0.1% MXene nanofluid performed greater heat transfer rate compared to 0.01% and 0.05% vol. concentration; although MXene nanofluids at various vol. concentrations (0.01%, 0.05%,

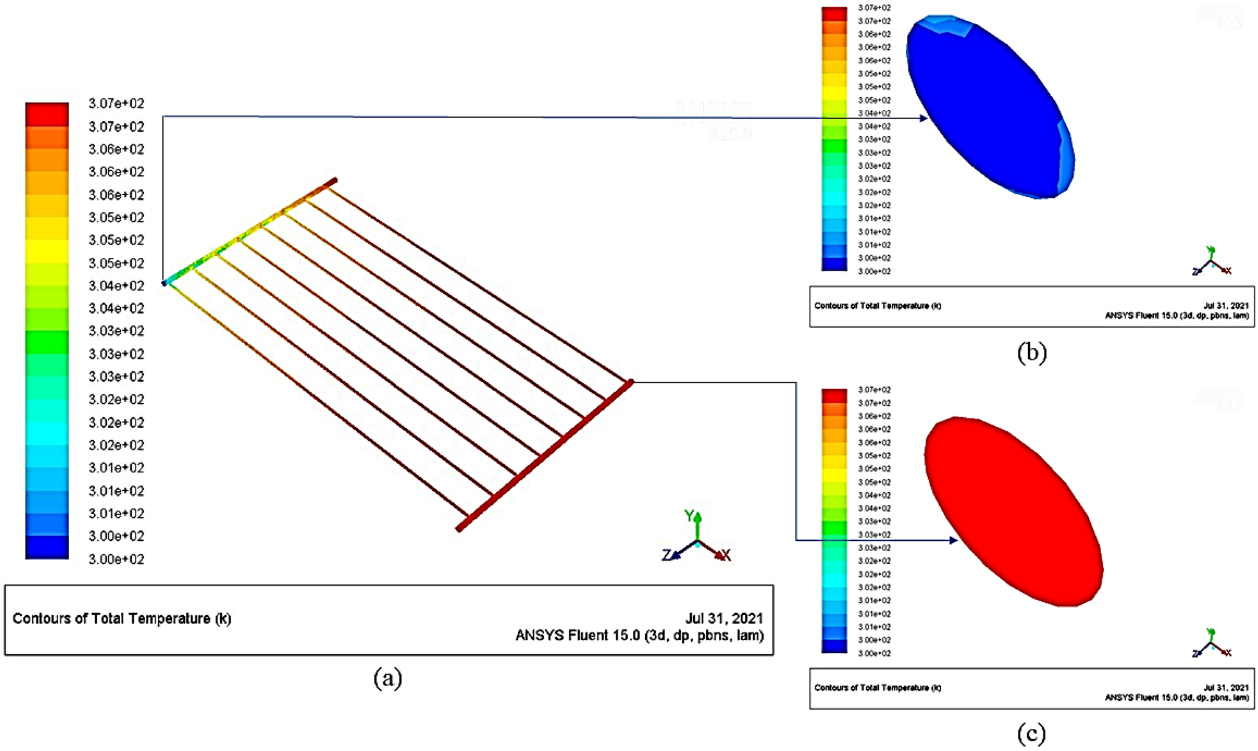

Fig. 5 Contour of the temperature of solar collector for MXene nanofluid

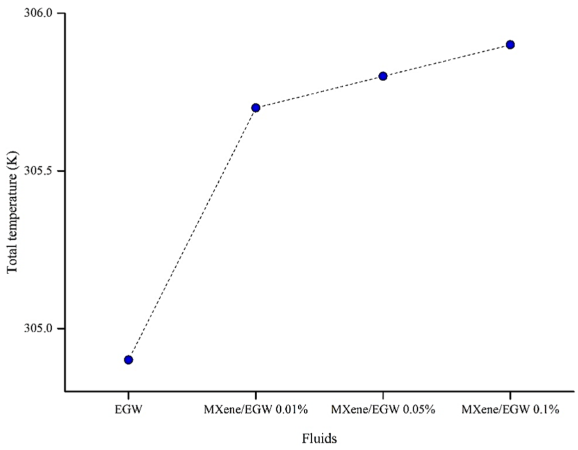

Fig. 6 Schematic presentation of temperature improvement of MXene nanofluids

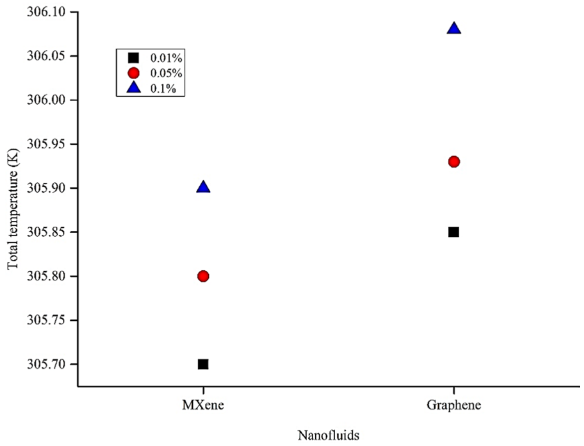

Fig. 7 Comparison analysis of temperature between MXene and graphene nanofluids

0.1%) showed the higher heat transfer rate contrasting with base fluid (Fig. 8) as well. The analogical performance of both types (MXene and graphene) of nanofluids has been shown in Fig. 9 which narrates the distinctive property of heat transfer rate between them. MXene nanofluids at 0.01%, 0.05%, 0.1% vol. con. illustrated positive direction enhanced heat transfer rate concerning graphene nanofluids with complementary vol. con. However, 0.05% vol. con. of graphene nanofluid demonstrated a negative direction of heat transfer (Fig. 9). This scenario is very parallel with one of the previous studies by Mahamude et al., (2021). On the other side of the coin, the surface heat transfer coefficient attribute of MXene nanofluids at varied volume concentrations performed lower performance compared to base fluid as presented in Fig. 10. However, the

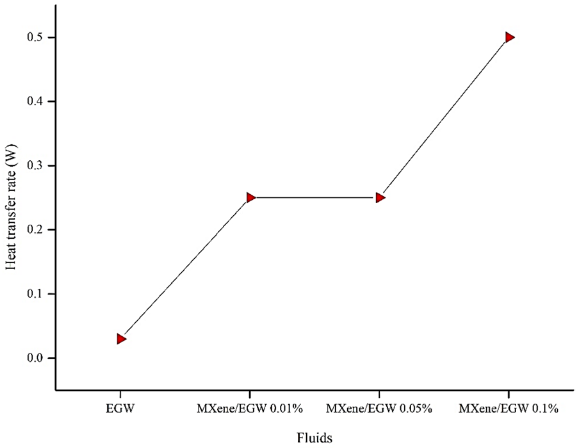

Fig. 8 Schematic presentation of the heat transfer rate of MXene nanofluids

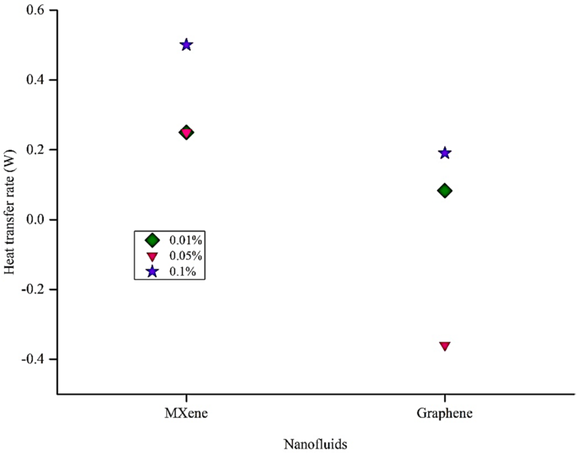

Fig. 9 Analogy of heat transfer rate of MXene nanofluids concerning other nanofluids

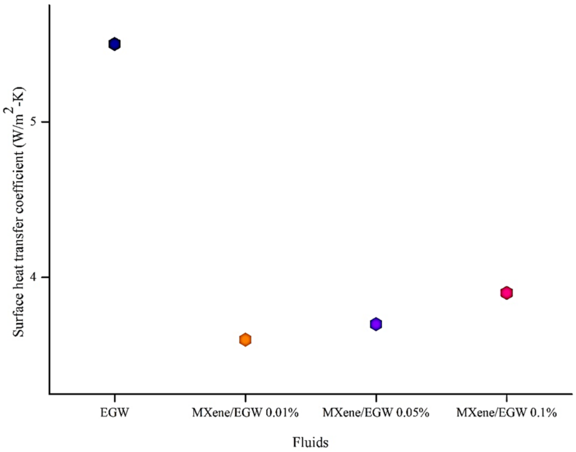

Fig. 10 Demonstration of surface heat transfer coefficient of MXene nanofluids

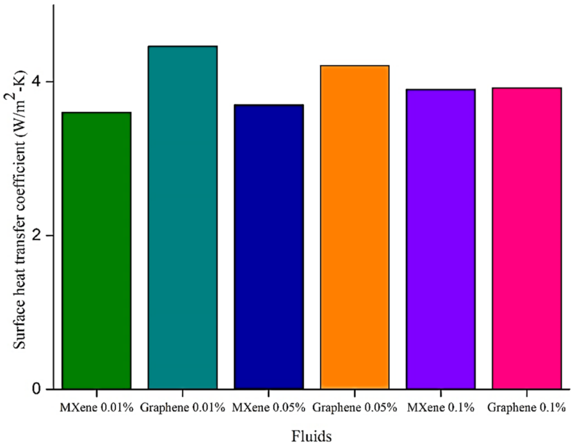

Fig. 11 Resemblance of MXene and graphene nanofluids in surface heat transfer coefficient

scenario shows showing opposite characteristics to the study of Mahamude et al., (2021); therein, nanofluids presented a higher surface heat transfer coefficient than base fluid. These could be happened due to MXene and other nanoparticles acquiring completely different characteristics and nanoparticles are minuscule objects and occupy unpredictable behaviour as well (Heiligtag & Niederberger, 2013). MXene nanofluids also depict that increasing volume concentration that signifies the surface heat transfer accordingly (Fig. 10). In an analytical study, MXene nanofluids portray a rising trend of surface heat transfer coefficient with an increased loading percentage of MXene nanoparticles into the base fluid as displayed in Fig. 11. However, graphene exhibited the opposite attitude with the same vol. con. compared to the surface heat transfer coefficient of MXene nanofluids. Graphene depicted a declining trend due to the escalation of the vol. con. of nanofluids. Herein, the final analytical criterion was skin friction coefficient (C_f) which is an imperative parameter of nanofluids for fluid flow. MXene nanofluids interpret a greater skin friction coefficient attitude at varied volume fractions compared with base fluid. Furthermore, they describe the positivity approach with the flow direction, as illustrated in Fig. 12. This characterizes quite relevant behaviour with our other studies, such as Mahamude et al., (2021) and Farhana, Kadirgama, and Noor (2021). However, 0.05% and 0.1% volume concentration MXene nanofluids performed the resemblance skin friction coefficient attribute in the solar collector. The observation study of the skin friction coefficient between MXene and graphene is demonstrated in

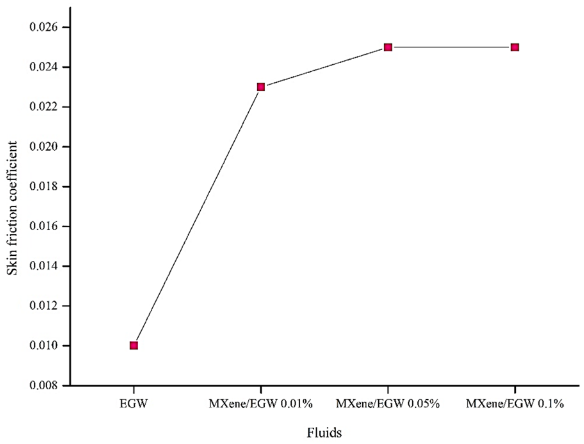

Fig. 12 Skin friction coefficient of MXene nanofluids in the solar collector

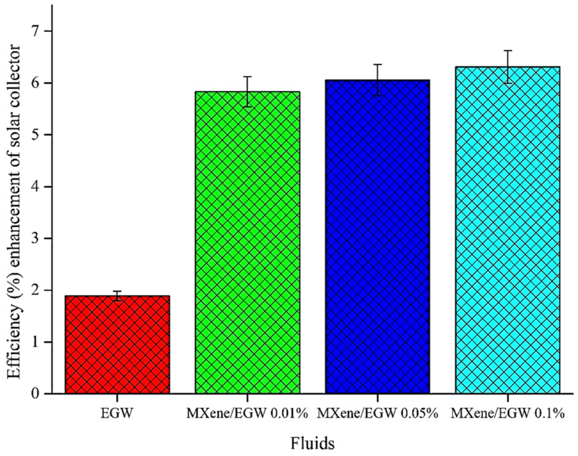

Fig. 14 Efficiency enhancement using MXene nanofluids in the solar collector

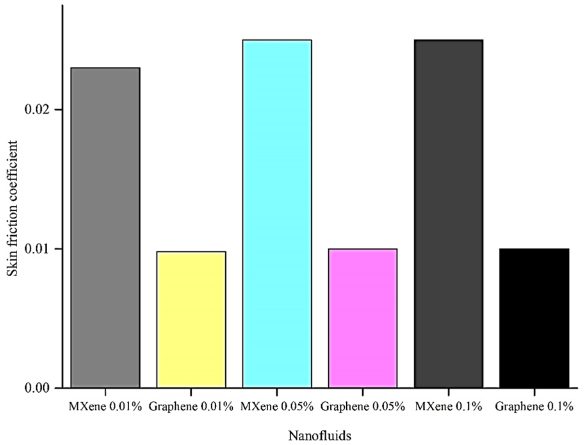

Fig. 13 Relation of skin friction coefficient of MXene and graphene nanofluids

Table 5 Comparison analysis between MXene and graphene nanofluids

Nanofluids	Temperature	Heat transfer rate	Surface heat transfer coefficient	Skin friction coefficient
MXene	–	Improved more than graphene	–	Improved more than graphene
Graphene	Increased higher than MXene	–	Increased higher than MXene	–

Fig. 13. 0.05% and 0.1% vol. con. of MXene nanofluids performed alike skin friction coefficient, whereas 0.01% showed a bit lesser performance. In contrast, graphene nanofluids with various vol. con. displayed a constant trend among them (Fig. 13). To acquire a full understanding of the differences between these two nanofluids, a summary of the comparison of the properties of MXene and graphene, including temperature, heat transfer rate, surface heat transfer coefficient, and skin friction coefficient, is drawn in Table 5. Table 5 presents that Mxene nanofluids exhibited higher performance in heat transfer rate and skin friction coefficient than graphene nanofluids. On the other side, graphene nanofluids showed better results than MXene nanofluids in case of outlet temperature and surface heat transfer coefficient.

The efficacy of the solar collector is illustrated in Fig. 14. In this study, efficiency has been surged using MXene nanofluids to replace conventional base fluid (EGW). Diverse volume concentrations such as 0.01%, 0.05%, and 0.1% of MXene nanofluids demonstrate the diversified efficiency enhancement of solar collectors. Figure 14 also depicts the gradual improvement of efficiency with increasing volume fractions of MXene nanoparticles into the base fluid with marginal error. Amongst them, 0.1% volume concentration determines the maximum efficiency of about 6.31% compared to base fluid followed by 6.06% at 0.05% and 5.83% at 0.01% volume weight of MXene nanofluids, respectively, while base fluid (EGW) exhibits 1.82% enhancement of efficiency of solar collector. The enhancement of efficacy of the solar collector by MXene nanofluid depends on various thermophysical parameters of nanofluids. Among them, thermal conductivity plays the main role in enhancing efficiency as increasing thermal conductivity boosts the heat transfer rate (Fig. 8) which consequently raises the outlet temperature (Fig. 6) as well (Farhana, Kadirgama, Rahman, et al., 2019a, 2019b, 2019c). The thermal conductivity of nanofluids is a crucial part of the increment of the heat transfer rate as a result of increasing outlet temperature and thermal efficacy as well. The notion of Brownian motion can be used to describe the thermal conductivity increase pattern. At greater temperatures, the particle collisions became more intense, increasing Brownian diffusion and reinforcing the increase in thermal conductivity (Farhana et al., 2021a, 2021b; Wen & Ding, 2004). Thereby, MXene nanofluids exhibited excellent thermal conductivity and displayed quite better other thermal properties numerically. As a consequence, the thermal efficacy of FPSC increased significantly empirically as well.

Conclusion

MXene nanoparticles dispersed in base fluid (Ethylene glycol–water) for efficiency enhancement of solar collector goal has been investigated. MXene nanofluids at 0.01%, 0.05%, and 0.1% volume concentration with an inlet mass flow rate of 0.0083 kg/s have been preferred. Some important points have been figured out as mentioned below:

- A better range of outlet temperature improvement was obtained than the base fluid. Consequently, excellent efficiency enhancement was achieved at about 5.83%, 6.06%, and 6.31% for 0.01%, 0.05%, and 0.1% volume fraction of nanofluids, respectively.
- The highest heat transfer rate was achieved by a 0.1% vol. concentration of MXene nanofluids of around 0.5 W.
- Maximum efficiency obtained by 0.1% vol. fraction of MXene nanofluids of about 0.32%.

The analysis shows that MXene nanoparticles can be applied in the solar collector for efficiency improvement purposes. Using this kind of heat transfer nanofluids to replace conventional working (base fluid) fluids can help in expanding more advanced flat plate solar collectors and can be used in other heat transfer applications as well.

Application in industry

This study will aid in understanding the application behavior of newly invented nanoparticles in the sustainable energy field. The research study will provide a new platform to reintroduce conventional working fluids to enhance the efficacy of solar harvesting devices. In general, solar collectors are used to heat the water in any kind of industry (Textiles, pharmaceuticals, etc.), home usage, and commercial buildings (Said et al., 2022). However, there are many obstacles to applying nanofluids in industrial applications and MXene is also not apart from them, such as nanofluid stability, nanoparticle size and volume fraction, viscosity of nanofluids, pumping power and pressure drop, cost of nanofluids, corrosion and erosion of nanofluids.

List of symbols

CFD	Computational fluid dynamics
CNC	Crystal nano-cellulose
EGW	Ethylene Glycol Water
FPSC	Flat plate solar collector
C_f	Skin friction coefficient
W	Water
ρ	Density (kg/m^3)
k	Thermal conductivity (W/m–K)
ϕ	Volumetric concentration of particles (%)
μ	Viscosity (kg/m. s)
v	Velocity (m/s)
C_p	Specific heat (J/kg-K)
w	Mass fraction
Q_u	Energy gain (kW)
$\dot{m}$	Mass flow rate (kg/s)
I_t	Incident solar radiation (W/m^2)
A_c	Area of the solar collector (m^2)
η	Efficiency (%)
T	Temperature (K)
p	Pressure (kg/m. s^2)
g	Gravitational acceleration (m/s^2)
h	Sensible enthalpy (joule)
∇	Advection operator

Subscripts

Nf	Nanofluid
Np	Nanoparticle
Bf	Base fluid

Acknowledgements
The authors are showing their gratitude to the University Malaysia Pahang for assisting with the grant numbers RDU213308 and RDU192208.

Author contributions

KF designed the concept, writing—original draft, data accumulation, data analysis, reviewing, and editing; ASFM data checking and writing; KK overall supervision, funding resources, editing, and checking; RJ overall supervision and funding resources.

Funding
Financial support by Bangabandhu Fellowship Trust and University Malaysia Pahang (UMP) provides the grants numbered RDU213308 and RDU192208.

Availability of data and materials

Data sharing does not apply to this article as no data sets were generated or analysed during the current study.

Declarations

Ethics approval and consent to participate

This study does not involve human participants. Therefore, ethics approval and consent to participate are not applicable.

Consent for publication

As this study does not include any identifying information of participants, consent for publication is not applicable.

Competing interests

The authors declare that they have no known competing financial interests or personal relationships that could have appeared to influence the work reported in this paper.

Received: 11 September 2023 Accepted: 17 November 2023

References

Abu-Hamdeh, N. H., Alazwari, M. A., Salilih, E. M., Sajadi, S. M., & Karimipour, A. J. (2021). Improve the efficiency and heat transfer rate'trend prediction of a flat-plate solar collector via a solar energy installation by examine the titanium dioxide/silicon dioxide-water nanofluid. *Sustainable Energy Technologies and Assessments, 48*, 101623.

Ahmadlouydarab, M., Ebadolahzadeh, M., & Ali, H. M. J. P. A. S. M. (2020). Effects of utilizing nanofluid as working fluid in a lab-scale designed FPSC to improve thermal absorption and efficiency. *Physica a: Statistical Mechanics and Its Applications, 540*, 123109.

Ahmadlouydarab, M., Anari, T. D., & Akbarzadeh, A. J. (2022). Experimental study on cylindrical and flat plate solar collectors' thermal efficiency comparison. *Renewable Energy, 190*, 848–864.

Aslfattahi, N., Loni, R., Bellos, E., et al. (2021). Efficiency enhancement of a solar dish collector operating with a novel soybean oil-based-MXene nanofluid and different cavity receivers. *Journal of Cleaner Production, 317*, 128430.

Bagherian, M. A., & Mehranzamir, K. J. (2020). A comprehensive review on renewable energy integration for combined heat and power production. *Energy Conversion and Management Science, 224*, 113454.

Borode, A., Ahmed, N., & Olubambi, P. J. (2019). A review of solar collectors using carbon-based nanofluids. *Journal of Cleaner Production, 241*, 118311.

Chen, L., Shi, X., Yu, N., et al. (2018). Measurement and analysis of thermal conductivity of Ti3C2Tx MXene films. *Materials, 11*(9), 1701.

Chu, S., Cui, Y., & Liu, N. (2017). The path towards sustainable energy. *Nature Materials, 16*(1), 16.

Davarnejad, R., & Jamshidzadeh, M. J. E. S. (2015). CFD modeling of heat transfer performance of MgO-water nanofluid under turbulent flow. *Engineering Science Technology, an International Journal, 18*(4), 536–542.

Farhana, K., Kadirgama, K., Rahman, M., et al. (2019b). Improvement in the performance of solar collectors with nanofluids—A state-of-the-art review. *Nano-Structures & Nano-Objects, 18*, 100276. https://doi.org/10.1016/j.nanoso.2019.100276

Farhana, K., Kadirgama, K., Ramasamy, D., Samykano, M., & Najafi, G. (2020). Experimental Studies on Thermo-Physical Properties of Nanocellulose-Aqueous Ethylene Glycol Nanofluids. *Journal of Advanced Research in Materials Science, 69*(1), 1–15.

Farhana, K., Kadirgama, K., Mohammed, H. A., et al. (2021a). Analysis of efficiency enhancement of flat plate solar collector using crystal nano-cellulose (CNC) nanofluids. *Sustainable Energy Technologies and Assessments, 45*, 101049. https://doi.org/10.1016/j.seta.2021.101049

Farhana, K., Kadirgama, K., & Noor, M. (2021b). *Analysis of non-dimensional numbers of fluid flowing inside tubes of flat plate solar collector advances in mechatronics, manufacturing, and mechanical engineering* (pp. 121–131). Berlin: Springer.

Farhana, K., Kadirgama, K., Mahamude, A. S. F., & Jose, R. (2023). Review of MXenes as a component in smart textiles and an adsorbent for textile wastewater remediation. *Chinese Chemical Letters*. https://doi.org/10.1016/j.cclet.2023.108533

Farhana, K., Kadirgama, K., Noor, M., et al. (2019). CFD modelling of different properties of nanofluids in header and riser tube of flat plate solar collector. Paper presented at the IOP Conference Series: Materials Science and Engineering.

Farhana, K., Mahamude, A., Kadirgama, K., et al. (2019). Internal energy analysis with nanofluids in header and riser tube of flat plate solar collector by CFD modelling. *Paper presented at the IOP Conference Series: Materials Science and Engineering*.

Fernández-García, A., Zarza, E., Valenzuela, L., & Pérez, M. J. (2010). Parabolic-trough solar collectors and their applications. *Renewable and Sustainable Energy Reviews, 14*(7), 1695–1721.

Genc, A. M., Ezan, M. A., & Turgut, A. J. (2018). Thermal performance of a nanofluid-based flat plate solar collector: A transient numerical study. *Applied Thermal Engineering, 130*, 395–407.

Goodarzi, M., Safaei, M., Vafai, K., et al. (2014). Investigation of nanofluid mixed convection in a shallow cavity using a two-phase mixture model. *International Journal of Thermal Sciences, 75*, 204–220.

Heiligtag, F. J., & Niederberger, M. J. M. T. (2013). The fascinating world of nanoparticle research. *Materials Today, 16*(7–8), 262–271.

Koziel, S., & Yang, X.-S. (2011). *Computational optimization, methods and algorithms* (Vol. 356). Berlin, Heidelberg: Springer.

Li, X., Chang, H., Zeng, L., et al. (2020). Numerical analysis of photothermal conversion performance of MXene nanofluid in direct absorption solar collectors. *Energy Conversion and Management Science, 226*, 113515.

Liu, R., & Li, W. (2018). High-thermal-stability and high-thermal-conductivity Ti3C2T x MXene/Poly (vinyl alcohol)(PVA) composites. *ACS Omega, 3*(3), 2609–2617. https://doi.org/10.1021/acsomega.7b02001

Mahamude, A. S. F., Harun, W. S. W., Kadirgama, K., et al. (2022). Experimental study on the efficiency improvement of flat plate solar collectors using hybrid nanofluids graphene/waste cotton. *Energies, 15*(7), 2309. https://doi.org/10.3390/en15072309

Mahamude, A. S. F., Harun, W. S. W., Kadirgama, K., Farhana, K., & Ramasamy, D. (2021). Numerical Studies of Graphene Hybrid Nanofluids in Flat Plate Solar Collector. Paper presented at the 2021 International Congress of Advanced Technology and Engineering (ICOTEN).

Mazumder, Q. H. (2012). CFD analysis of single and multiphase flow characteristics in elbow. *Engineering, 4*(04), 210.

Naguib, M., Kurtoglu, M., Presser, V., et al. (2011). Two-dimensional nanocrystals produced by exfoliation of Ti3AlC2. *Advanced Materials, 23*(37), 4248–4253.

Rehan, M. A., Ali, M., Sheikh, N. A., et al. (2018). Experimental performance analysis of low concentration ratio solar parabolic trough collectors with nanofluids in winter conditions. *Renewable Energy, 118*, 742–751.

Rubbi, F., Habib, K., Saidur, R., et al. (2020). Performance optimization of a hybrid PV/T solar system using Soybean oil/MXene nanofluids as A new class of heat transfer fluids. *Solar Energy, 208*, 124–138. https://doi.org/10.1016/j.solener.2020.07.060

Sahin, A. Z., Uddin, M. A., Yilbas, B. S., & Al-Sharafi, A. J. (2020). Performance enhancement of solar energy systems using nanofluids: An updated review. *Renewable Energy, 145*, 1126–1148.

Said, Z., Ghodbane, M., Boumeddane, B., et al. (2022). Energy, exergy, economic and environmental (4E) analysis of a parabolic trough solar collector using MXene based silicone oil nanofluids. *Solar Energy Materials and Solar Cells, 239*, 111633.

Sajid, M. J. (2020). MXenes: Are they emerging materials for analytical chemistry applications?–a review. *Analytica Chimica Acta., 1143*, 267.

Samylingam, L., Aslfattahi, N., Saidur, R., et al. (2020). Thermal and energy performance improvement of hybrid PV/T system by using olein palm oil with MXene as a new class of heat transfer fluid. *Solar Energy Materials and Solar Cells, 218*, 110754. https://doi.org/10.1016/j.solmat.2020.110754

Shekhirev, M., Shuck, C. E., Sarycheva, A., & Gogotsi, Y. J. (2021). Characterization of MXenes at every step, from their precursors to single flakes and assembled films. *Progress in Materials Science, 120*, 100757.

Sorokes, J. M., Hardin, J., Hutchinson, B. (2016). A CFD Primer: What Do All Those Colors Really Mean? Paper presented at the Proceedings of the 45th Turbomachinery Symposium.

Sreedhar, A., & Noh, J.-S.J. (2021). Recent advances in partially and completely derived 2D Ti3C2 MXene based TiO2 nanocomposites towards photocatalytic applications: A review. *Solar Energy, 222*, 48–73.

Verma, S. K., Gupta, N. K., & Rakshit, D. J. (2020). A comprehensive analysis on advances in application of solar collectors considering design, process and working fluid parameters for solar to thermal conversion. *Solar Energy, 208*, 1114–1150.

Wen, D., & Ding, Y. (2004). Experimental investigation into convective heat transfer of nanofluids at the entrance region under laminar flow conditions. *International Journal of Heat and Mass Transfer, 47*(24), 5181–5188. https://doi.org/10.1016/j.ijheatmasstransfer.2004.07.012

Yadav, J., & Singh, B. R. J. (2011). Study on performance evaluation of automotive radiator. *SAMRIDDHI A Journal of Physical Sciences, Engineering and Technology, 2*(02), 47–56.

Yin, J., Wei, K., Zhang, J., et al. (2022). MXene-based film electrode and all-round hydrogel electrolyte for flexible all-solid supercapacitor with extremely low working temperature. *Cell Reports Physical Science, 3*, 100893.

Yusaf, T., Mahamude, A. S. F., Farhana, K., et al. (2022). A comprehensive review on graphene nanoparticles: Preparation, properties, and applications. *Sustainability, 14*(19), 12336.

Zaman, K., & Abd-el Moemen, M. (2017). Energy consumption, carbon dioxide emissions and economic development: Evaluating alternative and plausible environmental hypothesis for sustainable growth. *Renewable and Sustainable Energy Reviews, 74*, 1119–1130.

Publisher's Note